Draft version July 11, 2025
Typeset using LaTeX **twocolumn** style in AASTeX7.0.1

1929 RO Orbit Determination

Ethan Li, Iris Luo, Skylar Kang[1]

[1] *SSP International Inc.*

(Dated: June 2025)

ABSTRACT

Classified by their distance from Mars' orbit, Mars-crossing asteroids (MCAs) potentially hold valuable clues in the study of asteroid migration, and potentially the migration to Earth's orbit. Knowing this, our study focuses on the orbital determination of the MCA 1929 RO, also known as the 1131 Porzia. Using three nights of observed data, intricate lines of Python code, multiple mathematical procedures, and standard image processing methods, the asteroid's orbital elements, positional changes, and a range of uncertainty can be concluded. Furthermore, the results of this study can be compared to a more precise source, such as JPL Horizons. However, there might be certain differences due to computational errors such as rounding. To combat these differences, the JPL values are referenced and their standard deviations are acknowledged. In this study, the orbital elements were calculated to be ranging from a 0.005769% - 3.448269% difference from our calculations and JPL Horizon's. and from this we can conclude our calculations will likely be relatively similar to computer calculated sources such as JPL Horizons. The study of MCAs are essential in providing data that may aid in the orbital prediction of other minor cosmic bodies. Perhaps, even potentially preventing a collision with Earth and a migrated asteroid.

1. INTRODUCTION

Mars-crossing asteroids (MCAs), form a transient group of asteroids which originate in the main asteroid belt that eventually migrate into near-Earth space or are flung onto hyperbolic trajectories.2023Icar..39415398F This dynamical group is especially intriguing because, as they escape the belt, they are highly likely to become Near-Earth Asteroids (NEAs)—defined as objects whose perihelion distance falls below 1.3 au.(J. A. Fernández & M. Helal 2023) This transformation from (MC) asteroids into (NEAs) is important because of the relatively close distance from Earth, which potentially risks disaster.

On average, MCA asteroids intersect the Earth's orbit for about 60 Myr(P. Michel et al. 2000). Then, they can switch between Earth-crossing and Mars-crossing before colliding with the Sun or being ejected outside Saturn's orbit (P. Michel et al. 2000). Previous studies have analyzed Mars-crossing asteroids over long periods of time(I. Wlodarczyk 2021). After simulations of hundreds of millions of years, it is found that approximately 66 % of MCA asteroids will exit the solar system due to collisions with various celestial objects(I. Wlodarczyk 2021). However, analyzing Mars-crossing asteroids over their orbit around Earth is fundamental to determining their relationship and any possible future interactions with Earth.

By using only three observations and a method which would later be named for him((C. Lue 2020)), the astronomer Carl Friedrich Gauss re-won Ceres, the newly discovered dwarf planet, in the early 19th century. Gauss's ingenious algorithm has survived to the present day and serves as the bedrock of modern asteroid orbit determination — especially for preliminary orbit computation from incomplete position data((E. Bowell et al. 2002)). At present, with the wide-field surveys detecting more and more near-Earth and Mars-crossing asteroids, there is renewed impetus regarding orbit-determination from sparse observations. Orbit determination has again taken on critical importance, both for planetary defense and to develop a better understanding of solar-system dynamics at large.

Research demonstrated very recently that Gauss's method is still applicable to modern examinations of asteroids. For instance, one of the publicly documented projects where Gauss's method was implemented was to calculate the orbit of Mars-crossing asteroid 10737 (1988 DZ4) from three observations taken over a period of about a month ((C. Lue 2020)). They constructed position and velocity vectors of the asteroid then refined the orbital elements using Monte Carlo simulations to provide a very preliminary orbit matching well with JPL ephemerides. Similar comparative works

((G. F. Gronchi et al. 2021)) have found out between Gauss's classical method and the recent ones, such as the Mossotti method((G. F. Gronchi et al. 2021)), that Gauss's original method is more reliable with respect to a wide range of synthetic asteroid datasets((N. P. D. System 2025)).

continuing in that tradition, this paper considers asteroid (720) Porzia, the Mars-crossing asteroid discovered in 1929, and focuses on simulating and refining the orbit of this particular body from a relatively sparse number of ground-based observations in Millegeville, Georgia.

The estimated diameter of Porzia is about 37 km, and its albedo is so low (0.05-0.07), indicating a relatively dark, carbonaceous composition. Although the mass and density combined are not well constrained, Porzia lends itself to an argument for significant gravitational perturbation from Mars through an indirect inference drawn from its moderate size and irregular shape. ((J. P. Laboratory 2025)) Porzia also has a higher level of eccentricity (0.25) and inclination (13°), and therefore, if it were to end up in a sort of dynamic regime, any change made with respect to velocity would immediately transform the trajectory, especially in very long-term orbits, which then raises the importance of initial orbit determination.

This research is not the the same kind of exercise as the 1988 DZ4, where the main goal was to check if the classical method was valid; rather, this work will make accuracy better by integrating the methods of Gauss with modern least-squares refinement and error propagation analysis. The aims of this paper are: The use of the Gauss method to determine Porzia's orbital elements from three independent astrometric measurements; simulation with numerical integration of its orbital path; Evaluation of sensitivity to measurement errors through Monte Carlo experiences; Finally, comparison of the emerging orbit with the ephemeris published (e. g. JPL Horizons) so that performance and limits of the method can be evaluated.

Such an approach would make it possible for the project to not only attempt to reproduce classical solutions to modern targets but also refute any arguments about the precision in orbit recovery, which would be important as we head into more autonomous and data-driven asteroid tracking in the future.

2. TARGET SELECTION

Porzia is a valid target for this study because it meets specific criteria optimal for observing. Its diameter measures at about 8.619 kilometers and is 0.59 AU from the closest point on Earth's orbit. Additionally, it has an elevation ranging from 38° - 42° during the observation window. Furthermore, Porzia has a magnitude ranging around 16, making it an observable asteroid. All of these factors add up to a valid target for this study. Moreover, because this study focuses explicitly on orbital path determination, the physical attributes of 1929 RO Porzia makes it a justifiable target.

3. OBSERVING METHODS

The data recorded in this study was collected at the Pohl Observatory at Georgia College and State University, which hosts an Aluma 8300 CCD and a PlaneWave CDK24 with a camera FOV of 12' x 16' ((G. College & S. University N.D.)). Data for the date's right ascension and Declination has been sourced from the Jet Propulsion Laboratory's Horizons System ((J. propulsion laboratory Horizons System N.D.)). Furthermore, star charts are sourced from Swarthmore's Annotated Finding Charts. Before each observation, we recorded the coordinates of Porzia using JPL Horizon Systems. Additionally, Swarthmore star charts are used as a tool of comparison. When observing, a series of flat, dark, and light images are taken. Each of these images serves a different purpose; however, when combined, they aid in producing sharp and clear images for analysis.

To complete our observations, SkyX is used to calibrate, focus, and monitor the telescope. After monitoring the telescope of the surroundings and the telescope, we input the RA and DEC into the input window and reposition the telescope and dome. We focus the telescope using an external application called the PWI Focus Tool and Temperature Monitor. Once everything is focused and suitable for taking images, we change our settings. Depending on the type of image being taken, there are different settings to use. For example, light images require 2x2 Binning, 5-second exposure, frame set to light and repeated to 12. During the two nights of observations at the Pohl Observatory, there are three 5-second images taken each night with a time interval of 10 minutes between each set. This is to ensure the movement and tracking of the asteroids. We also ensure that these images will save on our designated files.

4. IMAGE ANALYSIS

4.1. *Image Calibration*

To account for systematic errors and ensure clarity, several calibration steps are taken. During the first observation session on June 12th, around 2:00 AM - 3:15 AM UTC, a series of flatfields (0.100 second exposure), darks (0.100 second exposure), and later on, bias series were taken. These series are taken in order to be implemented in future processes of astrometry and photom-

etry. Additionally, 1929 RO will be detected with the aid of these initial series images. In the initial stages of image calibration, the main goal is to achieve a clean image suitable for analysis, the data were reduced and calibrated using standard methods. To prevent confusion, the UT date is consistently accounted for and maintained throughout calibration. This process of image calibration allows for the following steps in image analysis: astrometry and photometry.

4.2. *Astrometry*

The right ascension and declination of 1929 RO are determined through the centroiding-Least Squares Plate Reduction (LSPR) mechanism through Astronomy.net. Stacks are aligned to easily track and target the asteroid. Figure 1 shows the results of aligning and the location of the asteroid through 10 minute time-intervals. Background is first subtracted to ensure precision. Then, the center of the asteroid's flux distribution is precisely determined at the weighted mean for each pixel array axis, and the uncertainty is the standard deviation of the weighted mean on the subtracted background. Once centroided, the LSPR method is performed using a set of comparison stars that are clearly identifiable. Minimizing residuals from the best fit, the Cartesian coordinate is transformed to spherical coordinates. Accounting for background photons, the Right Ascension and Declination of the centroid is determined. Results are described in table 1.

Table 1. Right Ascension and Declination of 1929 RO for observing dates

Date	RA (H:M:S)	Dec (D:M:S)	Telescope	Exposure Time (s)
06-16	14 59 28.24	-13 34 50.0	PlaneWave CDK24	5
06-23	14 55 39.92	-13 34 34.0	PlaneWave CDK24	5
06-29	14 53 42.99	-13 40 02.1	0m4 SCICAM QHY600	60

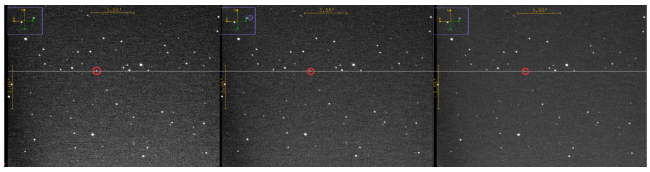

Figure 1. A 3 image time lapse of 1929 RO, circled in red, through 10-minute intervals taken on Day 2

4.3. *Photometry*

In order to resolve the apparent magnitude of 1929 RO, SAOImageDS9 is used to retrieve the asteroid's catalog through APASS. Images taken by both GCSU's observatory and LCOs are then compared in AIJ, and aperture photometry on the reference stars and 1929RO is performed by setting the radii (Inner radius, Radius, Outer Radius) to 10, 18, 22 pixels. Linear regression using log10(source-sky) as the x-axis and apparent magnitude of known/reference stars as the y-axis is performed to calibrate for the apparent magnitude of our asteroid. Plotting the log(source sky) of our asteroid on the line of best fit is used to find the magnitude. Additionally, the accuracy of observation time is ensured by adding half of the exposure time to the midpoint of observation.

Once image calibration is accomplished, the shift of the asteroid's position can be visually represented. Aside from the computational benefits, image calibration also shows the movement of the asteroid over the times of observations.

5. CALCULATIONS

5.1. *Gauss's Method*

In predicting the orbit of a heliocentric body such as an asteroid, the six orbital elements mentioned previously should be calculated. This can be done with Gauss's method. The independent variables for Gauss's method are the RA and DEC, times at which the asteroid was observed, and the position of the observer. These factors can be measured without any prior calculations and can be compared with data from JPL horizon.

Once these aspects are measured, RA and Dec are converted into vectors $\vec{rho}$ pointing from the observer to the asteroid. Summing this with the distance between the Earth and the sun $\vec{R}$, we obtain the heliocentric position vectors of the asteroid.

The ρ equations, are given as such:

$$\vec{\rho} = \vec{r} + \vec{R}$$

where

$$\rho_1 = \frac{\mathrm{a}_1 \left(\overrightarrow{\mathrm{R}}_1 \times \hat{\rho}_2\right) \cdot \hat{\rho}_3 - \left(\overrightarrow{\mathrm{R}}_2 \times \hat{\rho}_2\right) \cdot \hat{\rho}_3 + \mathrm{a}_3 \left(\overrightarrow{\mathrm{R}}_3 \times \hat{\rho}_2\right) \cdot \hat{\rho}_3}{\mathrm{a}_1 \left(\hat{\rho}_1 \times \hat{\rho}_2\right) \cdot \hat{\rho}_3}$$

$$\rho_2 = \frac{\mathrm{a}_1 \left(\hat{\rho}_1 \times \overrightarrow{\mathrm{R}}_1\right) \cdot \hat{\rho}_3 - \left(\hat{\rho}_1 \times \overrightarrow{\mathrm{R}}_2\right) \cdot \hat{\rho}_3 + \mathrm{a}_3 \left(\hat{\rho}_1 \times \overrightarrow{\mathrm{R}}_3\right) \cdot \hat{\rho}_3}{-\left(\hat{\rho}_1 \times \hat{\rho}_2\right) \cdot \hat{\rho}_3}$$

$$\rho_3 = \frac{\mathrm{a}_1\left(\hat{\rho}_2 \times \overrightarrow{\mathrm{R}}_1\right)\cdot\hat{\rho}_1 - \left(\hat{\rho}_2 \times \overrightarrow{\mathrm{R}}_2\right)\cdot\hat{\rho}_1 + \mathrm{a}_3\left(\hat{\rho}_2 \times \overrightarrow{\mathrm{R}}_3\right)\cdot\hat{\rho}_1}{\mathrm{a}_3\left(\hat{\rho}_2 \times \hat{\rho}_3\right)\cdot\hat{\rho}_1}$$

Furthermore, an essential step in our calculations is the f and g functions. These functions will iterate through our sets of "r" and "v" solutions for each night of data. The results of these iterations, dubbed as f_1, f_2, f_3, so on and so forth, can be used to continue the Method of Gauss. For example, the f and g values can be used to directly solve for a_1 and a_3, another set of variables needed to calculate the rest of Gauss' method.

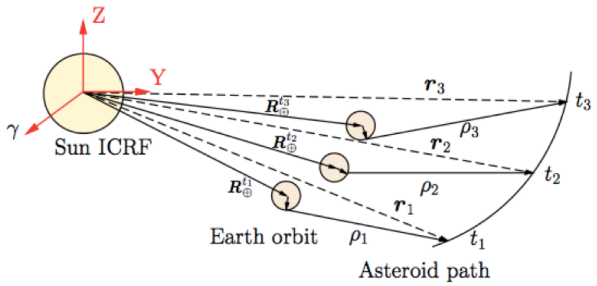

Figure 2. Relationship between $\vec{\rho}$, $\vec{r}$ and $\vec{R}$

5.2. *Orbital element calculation*

Then, the "r" (position) and "v" (velocity) vectors may be found from the previous system. Using standard formulas for the orbital elements, the vectors can now be inputted to find the six values. Using the position and velocity vectors calculated before, our orbital elements can be calculated. This section will provide an mathematical explanation of the equations and formulas used to find such elements using the vectors found. The vector h is defined as the angular momentum found from L = m r * v.

Semi-Major axis (a): $\frac{1}{\left(\frac{2}{r}-\frac{v^2}{\mu}\right)}$

Eccentricity(e): $\sqrt{1-\frac{h^2}{\mu * a}}$

Inclination(i): $\cos(i) = \frac{h_z}{h}$

The Longitude of the Ascending Node (Ω):

$\cos(\Omega) = \frac{h_y}{\sqrt{h_x^2+h_y^2}}$

Argument of Perihelion (ω): $w = u - \nu$

Where U is calculated by:

$cosU = \frac{r_x cos\Omega + r_y \sin\Omega}{r}$, $sinU = \frac{r_z}{r\sin i}$

Additionally, v is calculated by:

$cosv = \frac{1}{e}(\frac{a(1-e^2)}{r} - 1)$, $sinv = (\frac{a(1-e^2)}{eh})(\frac{\vec{r}\vec{r}}{r})$

Mean Anomaly (M): $M = E - e\sin E$

Where "E" stands in for the eccentric anomaly. Depending on which trig. function is used, the "r" and "v" vectors are applied to produce the eccentric anomaly value. Additionally, in (ω) calculations, "r" and "v' vectors are used in the trig. functions similar to Mean Anomaly calculations. Additionally, the "r" and "v" solutions are used the in the f and g functions of the Gauss method. These functions originate from the need to compare three nights of data. When iterating through the data of each night, these functions become useful in determining variables for future calculations.

5.3. *Uncertainty Estimation Method*

In our calculations, there is room for a range of uncertainty. This can be due to quite a few reasons, mainly during the numerical calculations and iterations coded for in Python. Computing the orbital elements were performed via Python following the equations of Kepler's laws, method of Gauss, etc. This was done to simplify and prevent mistakes when calculating the orbital elements for three different nights of data. However, using technology to calculate and especially iterate through multiple equations may cause some degree of variance from the actual observed elements. Uncertainty was calculated using the Monte Carlo method. Our .fits files are used to calculate the standard deviations of the RA and Dec for each night of observing according to $\sigma = \sqrt{\frac{\Sigma(x_f - x_i)^2}{N}}$.

This simulation is done in Python to reduce human error and conserve precision. A loop is implemented to determine a new RA and Dec value within the normal distribution stated by the original reported RA and Dec values. It is important to note that the Monte Carlo simulation is used specifically to report potential variations for our orbital determination elements. Knowing this, the Python code then completes the loop multiple times to report and store the produced orbital elements. This shows the potential uncertainty of the calculations of this study. Furthermore, histograms are created to provide a visual representation and comparison of our calculated elements compared to those recorded by JPL Horizons.

5.4. *Orbital elements results*

Table 2. Final results, Uncertainty, and JPL References

Element	Mean	JPL Value Mean	Units	Percent Difference%	Standard Deviation%
a	2.197387	2.228779	AU	1.408470	1.614692

Continued on next page

Table 2 – *continued from previous page*

Date	RA (H:M:S)	Dec (D:M:S)	Telescope	Exposure Time (s)	
e	0.275904	0.285758	None	3.448249	4.171641
i	3.229653	3.229839	Degrees	0.005769	0.390343
Ω	101.251561	100.650729	Degrees	0.596947	0.184736
ω	249.725145	248.043804	Degrees	0.677840	1.408743
M	285.746879	289.285188	Degrees	1.223122	1.830190

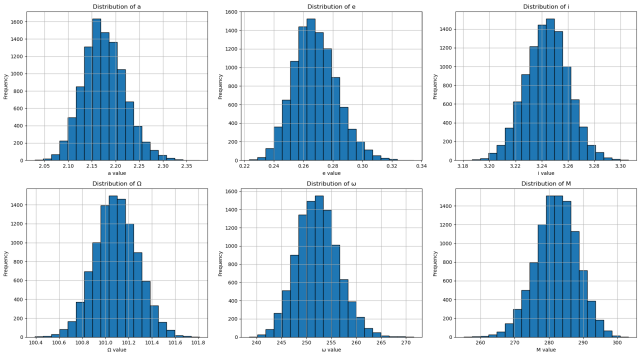

Figure 3. Monte Carlo Results

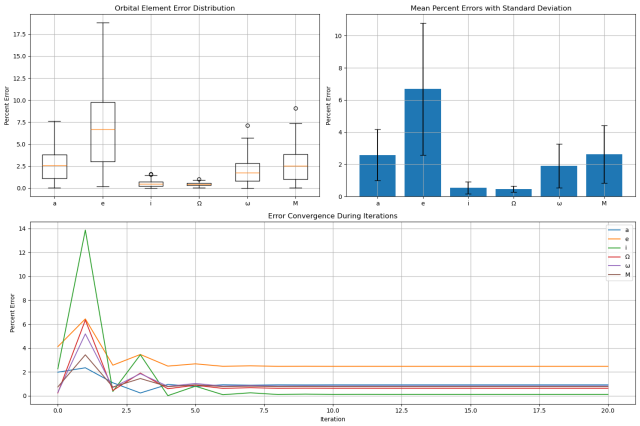

Figure 4. up-left:Distribution (median, IQR, outliers) of percent errors; up-right:Mean percent errors with standard deviations as whiskers; lower: error variation throughout iterations

These results show the orbital elements of the 1929 RO we have calculated. Referencing Table 2., it can be shown that our element values are relatively similar to JPL's reference values, with the percent difference ranging from 0.005769% - 3.448269%. These percentages are not of great significance, meaning, the results of our computations are roughly similar to the "modern" JPL values. Furthermore, we also ran a Monte Carlo simulation to account for uncertainty. The resulting histograms are shown in Figure 2. The distribution of the graph is roughly normal, signifying a degree of accuracy in our results, but also visually representing variance.

6. DISCUSSION

Although our code was as accurate as possible, and all orbital determination processes were followed intricately, there is still a possibility of error/uncertainty.

As a Mars-crossing asteroid, external perturbation from mars should contribute to errors in two-body trajectory simulation. Throughout the observation windows, the asteroid went from 1.9163AU to 2.0038AU from Mars, which exerts a force around 3.5043e+18N to 3.8313e+18N. This makes the asteroid accelerate towards Mars at approximately $4.768m \times 10^{-}4/s^2$to $5.213m \times 10^{-}4/s^2$.

Another potential error source might be the averaging of observation time. Since three series are taken each night, considering the uneven loading time for SkyX, the mean time of observation might not be exactly equal to the time of the second observation that we used as input in the code. These may explain the differences between the mean values of our results and of JPL's reference values, and efforts will be made in the future to optimize predictions.

7. REFLECTION

Ethan:

A word that I would sum up this project is worthwhile. Spending numerous days learning various complex algorithms, such as Newton-Raphson, and countless long nights completing my programming assignments has now finally shown its rewards. On every coding assignment, there always seemed to be an error that would take hours to figure out how to debug. However, looking back on all the struggles and justifiable crashouts, I really enjoyed the process. Having the lessons and assignments break the orbit determination into pieces was very beneficial, as grasping a conceptual understanding of the process was helpful to my success and the accurate generation of orbits. The feeling of completing a month-long project and seeing the ephemeris variables match JPL's variables was incredibly enjoyable, and I hope to experience that feeling again with future research.

I think I not only improved academically but also socially. Working with my team, Gang-A-Lang, has emphasized the importance of good communication and supporting the people around you and your team. There were times when I struggled with some coding or writing assignments, but collaborating with my team easily alleviated the issue.

Iris: This project taught me a hard lesson: small fluctuations, even at 6/7 decimal places, are fatal to simulation success. Having done multiple physics simulations before, I have approximated the size of bubbles without considering glass container magnification, entered placeholder values for better fitting line, etc. They made my result look pretty and made my research paper successful. Minor deviation from truth, to me, does not change the overall pattern. That perception changed when a small deviation of our data from the actual Julian date resulted in a prolonged error in calculation that resulted in a negative semi-major axis. Because of this, I struggled with the Monte Carlo simulation for 2 days, even though it works for every other dataset. Due to the approximation mentioned in the conclusion, I used the mean observation time as input. Turns out, the exact observation time could be seen from the AIJ file. After this realization, I revised the sun vectors according to the Julian date, and our code now runs perfectly. I will never make unreasonable assumptions and approximations thanks to this project.

Skylar: While working on the orbital determination project, there were many rewarding and challenging moments. For example, it was rewarding when my code ran correctly but it was challenging to even begin at first. That is also why some of the Python assignments went somewhat unexpectedly well because I managed to get the code to run. Still, to this day some assignments are still unfinished. I would say there was nothing that was an unexpected struggle because I expected everything to be a struggle. I believe I improved on a little bit of everything, still not at all proficient but it is more than I knew before. Also, as a group I think we improved on a lot of collaboration skills. Because I struggled on coding and performing image analysis, I focused on writing and our team collaborated to complete the project.

REFERENCES

Bowell, E., Virtanen, J., Muinonen, K., & Boattini, A. 2002, Asteroids III

College, G., & University, S. N.D., Observatory, https://www.gcsu.edu/observatory

Fernández, J. A., & Helal, M. 2023, Icarus, 394, 115398, doi: 10.1016/j.icarus.2022.115398

Gronchi, G. F., Baù, G., Rodríguez, , Jedicke, R., & Moeyens, J. 2021, Celestial Mechanics and Dynamical Astronomy, 133, doi: 10.1007/s10569-021-10038-4

Laboratory, J. P. 2025, JPL Small-Body Database Browser, https://ssd.jpl.nasa.gov/tools/sbdb_lookup.html#/?sstr=1131

Lue, C. 2020, Orbit-Determination,1988-DZ4, https://github.com/ChristopherLuey/Orbit-Determination-1988DZ4

Michel, P., Migliorini, F., Morbidelli, A., & Zappalà, V. 2000, Icarus, 145, 332, doi: 10.1006/icar.2000.6358

propulsion laboratory Horizons System, J. N.D., Jet propulsion laboratory Horizons System, https://ssd.jpl.nasa.gov/horizons/app.html#/

System, N. P. D. 2025, The Planetary Data System, https://pds.nasa.gov/

Wlodarczyk, I. 2021, MNRAS, 500, 3569, doi: 10.1093/mnras/staa3566